Applied Surface Science 255 (2009) 5674–5681

Contents lists available at ScienceDirect

Applied Surface Science

journal homepage: www.elsevier.com/locate/apsusc

Atypical grain growth for (2 1 1) CdTe films deposited on surface reconstructed (1 0 0) $SrTiO_3$ substrates

S. Neretina [a,1], R.A. Hughes [b,*], G.A. Devenyi [a,b], N.V. Sochinskii [c], J.S. Preston [a,b], P. Mascher [a]

[a] Department of Engineering Physics and Centre for Emerging Device Technologies, McMaster University, Hamilton, Ontario L8S 4L7, Canada
[b] Brockhouse Institute for Materials Research, McMaster University, Hamilton, Ontario L8S 4M1, Canada
[c] Instituto de Microelectronica de Madrid CNM – CSIC, Madrid 28760, Spain

ARTICLE INFO

Article history:
Received 9 March 2008
Received in revised form 7 November 2008
Accepted 21 December 2008
Available online 27 December 2008

PACS:
61.05.cp
61.72.Mm
61.72.uj
68.37.Ps
68.47.Gh
68.55.–a
68.55.A–

Keywords:
Surface reconstruction
Film
(211) CdTe
$SrTiO_3$
Steps and terraces
Miscut
Vicinal
$c(6 \times 2)$
$c(4 \times 2)$

ABSTRACT

The (1 0 0) $SrTiO_3$ substrate has emerged as the oxide substrate of choice for the deposition of a wide variety of materials. The substrate's unavoidable miscut leads to a step-terrace morphology when heated to high temperatures. This morphological transition is accompanied by an atomic scale repositioning of the uppermost terrace atoms, the nature of which is strongly dependent on the substrate temperature and ambient atmosphere used. Here, we report the deposition of CdTe films on the as-received and reconstructed surfaces of (1 0 0) $SrTiO_3$. The as-received substrate gives rise to a [1 1 1] CdTe film with four equally distributed in-plane grain orientations. The surface reconstruction, on the other hand, gives rise to an unprecedented reorientation of the film's grain structure. For this case, a [2 1 1] CdTe film emerges having twelve unevenly distributed in-plane orientations. We attribute the film's grain structure to an atomic scale surface reconstruction, with the anisotropic distribution of grain-types arising from a preferential formation due to the step edges.

1. Introduction

The surface of (1 0 0) $SrTiO_3$ has received considerable attention as its perovskite crystal structure presents a suitable template for the growth of a wide variety of oxide materials. This interest is largely due to the recognition of oxides as a class of materials that exhibits nearly every significant solid state phenomenon. With a toolbox of oxides that include dielectrics, ferroelectrics, piezoelectrics, relaxors, insulators, semiconductors, metals, high temperature superconductors, catalysts, photoluminescent materials, ferromagnets, ferrimagnets, antiferromagnets, diamagnets, and giant magnetoresistors, the potential exists for the emergence of oxide electronics that are capable of exploiting these properties on a stand-alone basis or by integrating them with conventional semiconductor devices. The emergence of $SrTiO_3$ as the substrate of choice is, to a large extent, a result of the epitaxial relationship achievable with numerous technologically significant oxides. It may also prove to be an effective means of linking oxide- and silicon-based technologies as the two materials are epitaxially compatible [1,2]. Further interest in this material stems from its ability to conduct electricity when doped with niobium [3], form a high mobility electron gas at an interface with $LaAlO_3$ [4,5] and photoluminesce upon oxygen reduction [6]. The use of miscut (1 0 0) $SrTiO_3$ substrates has further advanced its utilization both through the promotion of superior film quality, brought on by a step-flow growth mode [7–10] and as a means of promoting rows

* Corresponding author. Tel.: +1 905 5259140x23978; fax: +1 905 5212773.
E-mail address: hughesr@mcmaster.ca (R.A. Hughes).
[1] Present address: Georgia Institute of Technology, School of Chemistry and Biochemistry, 901 Atlantic Drive, Atlanta, GA 30332-0400, United States.

0169-4332/$ – see front matter © 2009 Elsevier B.V. All rights reserved.
doi:10.1016/j.apsusc.2008.12.050

of metallic nanoparticles along the step edges [11]. Coinciding with this research has been an extensive effort devoted to understanding the surface of (1 0 0) $SrTiO_3$.

The application of heat to a $SrTiO_3$ surface results in important reconstructions on two length scales. On an atomic scale, there is a local rearrangement of atoms that lowers the free energy of the surface relative to the bulk terminated surface. For the (1 0 0) $SrTiO_3$ surface there exist numerous reports detailing the possible reconstructions obtained at temperatures in excess of 800 °C. These measurements, largely based on low energy electron diffraction (LEED) and scanning tunneling microscopy, have shown the existence of seven reconstructions as well as a multitude of surface phases that are structurally variant to the bulk [12], where the formation of any given one is strongly dependent upon the annealing temperature and ambient used [13–21,16,22]. Before any such anneal is performed it is now commonplace to expose the substrate surface to a buffered-hydrofluoric (BHF) acid etch able to replace the mixed SrO/TiO_2 surface termination with a singly terminated TiO_2 surface [23–26]. For the oxidizing ambient relevant to our experiments, the (2×1), $c(4 \times 2)$, and $c(6 \times 2)$ reconstructions have been observed [14,16–18]. It should be noted that, while a significant range of reconstructions have been reported, in no case is bulk termination observed.

In addition to the atomic scale reconstruction described above, for a miscut surface, a step-terrace structure develops where the step geometry is strongly dependent upon the direction of the miscut [27–29]. For example, if the miscut is directed towards the in-plane [0 1 0] direction then a series of well defined and equally spaced steps form with the spacing between steps determined by the miscut angle. If the miscut is directed towards the in-plane [0 1 1] direction then the steps will exhibit a jagged saw-tooth morphology with the faces of the teeth pointing in the [0 1 0] and [0 0 1] directions. If the miscut lies between these two extremes then the steps will have a jaggedness, but of reduced significance. Thus, for all cases, the step edges expose the same crystallographic face as a nucleation site to a growing film.

Step-terrace structures have been widely employed to modify the growth dynamics by encouraging step-flow growth. The steps, typically one unit cell high, present excellent nucleation sites as adatoms are able to simultaneously bond to both the step and terrace. In the ideal scenario, identical grains emerge from the nucleation sites enabling a seamless coalescence of the grains as they merge to form a continuous film. Such a growth mode can be quite advantageous for situations where the heteroepitaxial relationship on a planar substrate gives rise to multiple grain orientations, compromising the film quality through the formation of grain boundaries. Here, the addition of steps provides a mechanism able to promote one grain orientation at the expense of another [7,10,30]. An important example is the growth of CdTe on (1 0 0) silicon [30–37] where in the absence of steps there exist four equivalent grain orientations. The introduction of a miscut, however, introduces one-dimensional step-terrace structures that break the four-fold symmetry of the surface. This measure, in combination with a tellurium monolayer pre-deposition, has resulted in the preferential formation of one specific grain type [30].

Previously we have deposited CdTe films on the as-received surface of (1 0 0) $SrTiO_3$ [38]. The grain structure observed was similar to CdTe on a (1 0 0) silicon substrate [30]. For both of these substrates, [1 1 1] CdTe films grow having four in-plane grain orientations that are in-sync with the four-fold symmetry of the substrate's surface. Motivated by the success obtained using silicon we have deposited CdTe films on miscut (1 0 0) $SrTiO_3$ substrates, where in an analogous manner, we break the four-fold symmetry of the surface through the formation of a step-terrace structure. Quite unexpected was that the resulting CdTe film had a [2 1 1] orientation. This new epitaxial relationship is consistent with the orientational relationship anticipated for the $c(6 \times 2)$ atomic scale reconstruction of the substrate's surface. As would be expected from geometric considerations, we observe twelve allowed orientations of the [2 1 1] oriented film on the $c(6 \times 2)$ reconstructed surface. The step-terrace structure is found to play an important role, however, in that it gives rise to the preferential nucleation of [2 1 1] grains that have their [1 1 1] direction normal to the step. This leads to a strong texturing of the final film with the degree of texturing dictated by the step density.

2. Substrate preparation and characterization

CdTe films were deposited on both the as-received and reconstructed surface of (1 0 0) $SrTiO_3$ (MTI Corporation). Step-terrace formation relied upon the miscut originating from the inaccuracies in the crystallographic alignment carried out prior to the cutting and polishing of the substrates (manufacturer's miscut tolerance $\leq 0.5^\circ$). As a result, the degree of miscut could only be varied through the use of substrates from different batches. Due to the high temperatures required, the surface reconstruction took place *ex situ* in a quartz tube furnace. Prior to annealing, the substrates were etched in BHF for 90 s. Anneals were conducted in flowing oxygen (60 cm^3/min) at 1000 °C for 10 h. Fig. 1 shows atomic force microscopy (AFM) images for the as-received and surface reconstructed substrates relevant to this work. As expected, only the annealed substrates exhibit the step-terrace structure with unit cell step heights. The difference in terrace width for the surfaces shown in Fig. 1b and c can be attributed to a miscut difference estimated at 0.35°. Also present on each image are the crystallographic axes obtained through X-ray diffraction (XRD). Note that a nearly identical in-plane step direction exists for both reconstructed surfaces. As this direction is close to, but not aligned with the [0 1 1] axis of $SrTiO_3$, it is expected that the steps exhibit a saw-tooth morphology, but on length scales not readily observed using atomic force microscopy.

3. CdTe film preparation and characterization

CdTe films were deposited on the three $SrTiO_3$ surfaces shown in Fig. 1 using the pulsed laser deposition technique. The laser used in this process was a GSI-Lumonics Ipex-848 excimer laser operating at 248 nm. The pulses, exciting the laser at an energy of 250 mJ, were passed through a rectangular mask to obtain the uniform central portion of the beam. The image of the mask was then focused onto a rotating CdTe target to a spot size of 1.5 mm × 3 mm yielding an energy density of 2 J/cm^2. The 1 in. diameter CdTe target was grown using the modified Bridgman method [39]. A deposition rate of 20 nm/min was achieved by operating the laser at a repetition rate of 10 Hz with a substrate to target distance of 3.5 cm. All films were deposited at 300 °C in vacuum with a base pressure of 6×10^{-7} Torr. Films were grown to a thickness of 300 nm as determined using a spectroscopic variable angle ellipsometer (Horiba Jobin Yvon, France). Morphological and structural characterization was then conducted on the films produced.

Fig. 2 shows the AFM images obtained for the CdTe films deposited on the surfaces shown in Fig. 1. Films deposited on all three substrates show the grain structure typical of an island growth mode. These images also make it immediately obvious that a reconstructed surface is able to dramatically alter the grain structure. Films deposited on the as-received surface exhibit a grain structure characterized by protrusions from the surface. The films deposited on the reconstructed surfaces, while still showing a grain structure, do so in a manner that results in a significant improvement in the mean roughness over the film deposited on

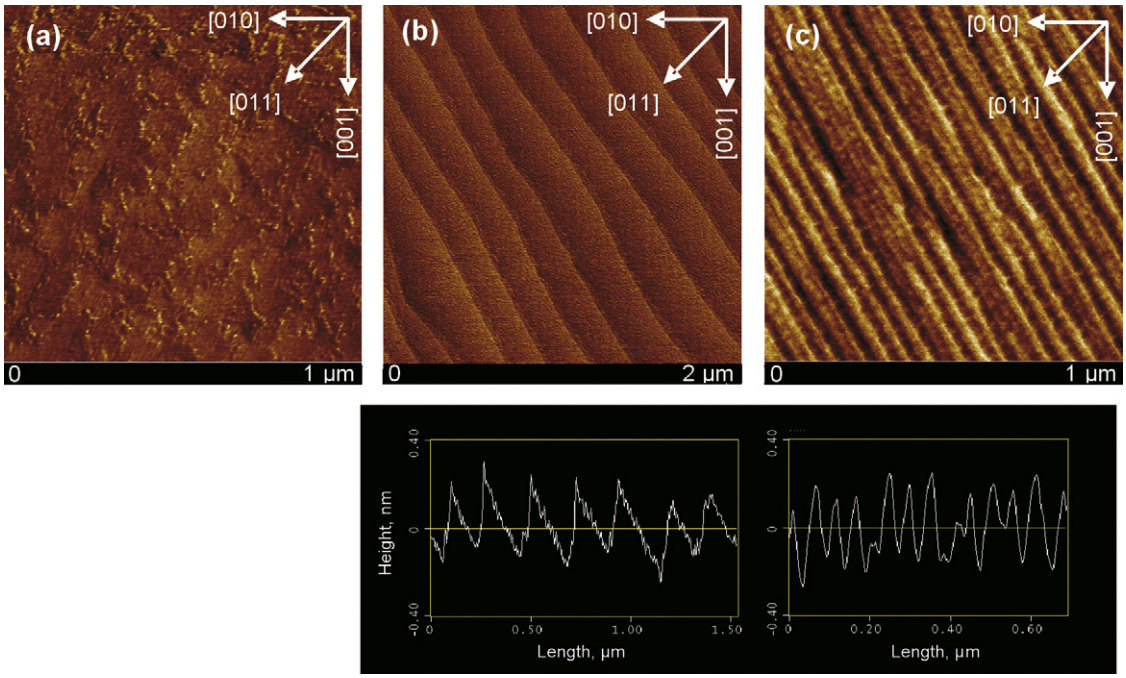

Fig. 1. AFM images for the (a) as-received (1 0 0) $SrTiO_3$ substrate, (b) a reconstructed surface with an average terrace width of approximately 200 nm and (c) a reconstructed surface with a terrace width of approximately 50 nm. From the step heights and terrace widths it is estimated that the miscuts for the two reconstructed surfaces are (b) 0.11° and (c) 0.46°. Below the images of the stepped surface are averaged surface profiles which clearly show the existence of unit cell surface steps. The images were obtained using a Digital Instruments Nanoscope III atomic force microscope (AFM) operating in tapping mode. Indicated on each image are the substrate's in-plane crystallographic axes obtained from XRD measurements. Note that the scale for the central image is twice that of the other two images.

the as-received surface. It should also be noted that the narrow terraced substrate gives rise to an average grain size of 0.03 μm^2 which is approximately 20% larger than that of the substrate with wider terraces.

Structural information was obtained using texture analysis made available through two-dimensional X-ray diffraction (2D-XRD) measurements. A Bruker SMART6000 CCD detector on a Bruker 3-circle D8 goniometer with a Rigaku RU-200 rotating anode X-ray generator and parallel-focusing mirror optics were used for the data collection. The data was obtained with the detector at −45° using two scans of two-second frames in 1° intervals: (1) a 360° φ-axis scan at $\omega = -185°$ and (2) a 40° ω-axis scan extending from −185° to −224° at $\varphi = 0°$. The surface of the sample was positioned at the optical center of the diffractometer,

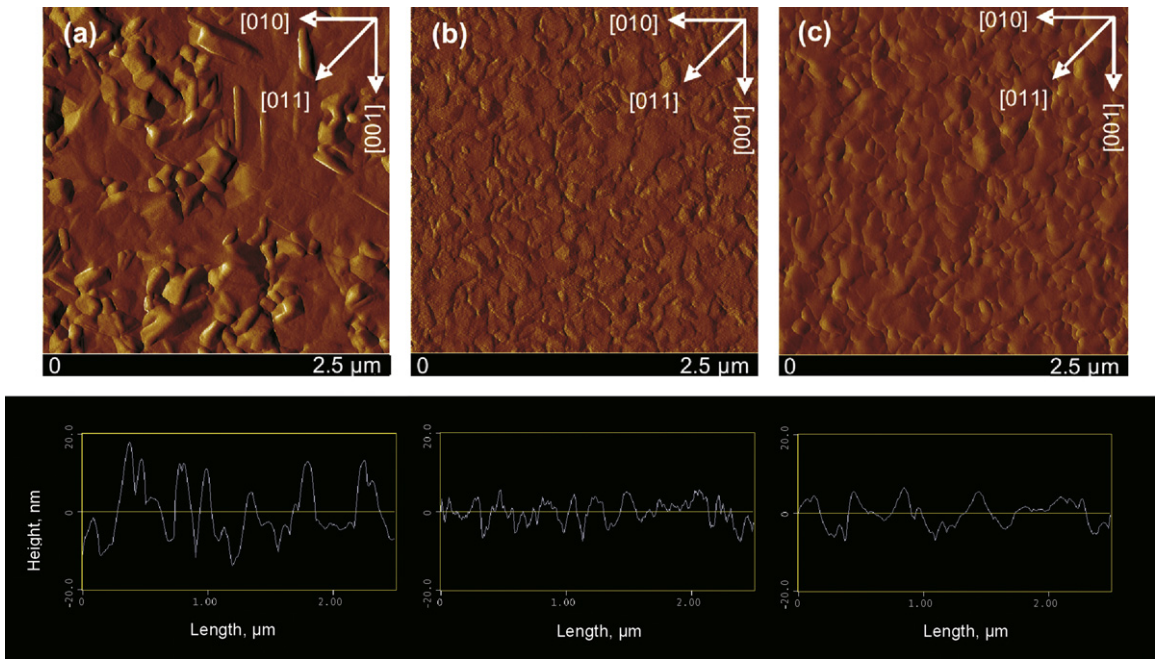

Fig. 2. AFM images and typical surface profiles for CdTe films deposited on (a) the as-received (1 0 0) $SrTiO_3$ substrate, (b) the reconstructed surface with wide terraces, and (c) the reconstructed surface with narrow terraces. The mean roughnesses for the three surfaces are (a) 6.1 nm (b) 4.2 nm and (c) 5.1 nm. Indicated on each image are the substrate's in-plane crystallographic axes obtained from XRD measurements.

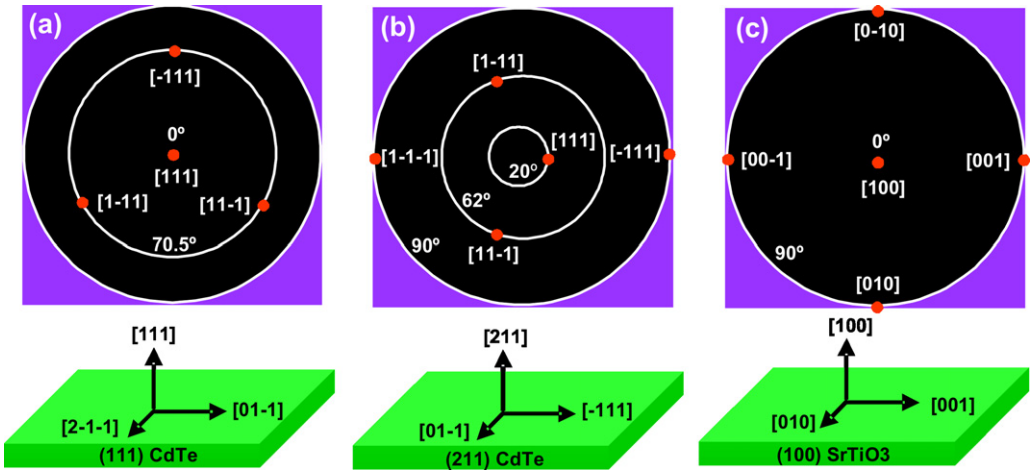

Fig. 3. Schematics showing the (1 1 1) pole figure expected for a single crystal CdTe film with a (a) [1 1 1] and (b) [2 1 1] orientation. (c) Schematic showing the (1 0 0) pole figure expected for a [1 0 0] oriented $SrTiO_3$ substrate. The normal and in-plane Miller indices are also shown for each case.

5.165 cm from the detector. Data collection was controlled with the SMART (Bruker-AXS) software and data analysis was performed with the GADDS (Bruker-AXS) package.

The data obtained allows for the generation of pole figures which are stereographic maps of the sample that pinpoint the real-space directions where a specific crystallographic periodicity lies. Because every crystallographic periodicity can be observed from above and below it is only necessary for the pole figures to map out the upper half of real-space. A peak at the center of the pole indicates those planes that are parallel to the surface while a peak at the edge of the pole corresponds to planes that are perpendicular. Intermediate values represent the possible orientations between these two extremes. Fig. 3 shows schematics of the three pole figures of relevance to this work. Fig. 3a shows the (1 1 1) pole figure for a single crystal [1 1 1] CdTe film. Here, the peak at the center of the pole corresponds to the [1 1 1] direction that points normal to the film's surface, while the three peaks closer to the edge of the pole correspond to the equivalent (−1 1 1), (1 −1 1) and (1 1 −1) planes that emerge at an angle of 70.5° with respect to the surface. For the single crystal [2 1 1] CdTe film shown in Fig. 3b, the same periodicities exist within the sample, but their positioning on the pole figure is altered. For this case, the (1 1 1) equivalent planes emerge from the film at an angle of 20°, 62° or 90° relative to the surface. Fig. 3c shows the (1 0 0) pole figure expected for a (1 0 0) $SrTiO_3$ substrate. Due to experimental limitations, peaks at 90° are experimentally unobservable. Also of significance is the fact that the (1 0 0) $SrTiO_3$ and (1 1 1) CdTe pole figures overlap as they have a nearly identical periodicity. Since only the central peak of the (1 0 0) pole figure is observable, the impact of this overlap on the (1 1 1) CdTe pole figure is minimal.

Fig. 4 shows the (1 1 1) CdTe pole figures for the three films shown in Fig. 2. The dramatic differences observed between films deposited on the as-received and annealed substrates indicate that the surface reconstruction gives rise to a complete re-alignment of the CdTe grains, an observation consistent with the measured surface morphologies. The pole figure for the as-received surface is consistent with a [1 1 1] oriented film. The fact that twelve peaks exist in the outer ring, instead of the three expected for a single crystal, indicates that there are four in-plane grain orientations. The pole figures for the films deposited on the surface reconstructed substrates show that both films are predominantly [2 1 1] oriented. The twelve peaks in the central ring and twenty-four peaks in the outer ring denote twelve in-plane grain orientations. It should be noted, however, that while each peak in the central ring corresponds to a unique grain orientation the peaks are of different intensity. This is a clear indication that some grains form preferentially over others. Note that of the twelve peaks both the strongest and weakest is in-line with the miscut direction for both of the reconstructed surfaces and that the degree of this preferential orientation is stronger for the reconstructed surface having the narrow terrace width. An examination of the low intensity pole figure peaks (not visible in the figures), indicates that some [1 1 1] CdTe grains exist in these nominally [2 1 1] films, but at the 10% percent level. While these [1 1 1] grains contribute to the intensity at the center of the pole, the response there is almost entirely due to the (1 0 0) $SrTiO_3$ substrate.

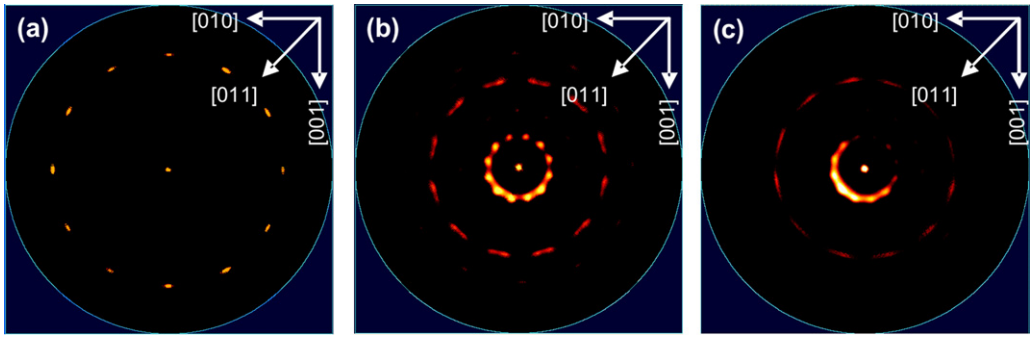

Fig. 4. (1 1 1) CdTe pole figures for films deposited on (a) the as-received (1 0 0) $SrTiO_3$ substrate (b) the reconstructed surface with wide terraces and (c) the reconstructed surface with narrow terraces. Indicated on each image are the substrate's in-plane crystallographic axes obtained from XRD measurements.

4. Discussion of results

Grain formation for a given film/substrate combination is determined by the interface energy. For the case of the as-received (1 0 0) $SrTiO_3$ substrate the interface energy is minimized through the formation of [1 1 1] CdTe grains. This interfacial relationship is not surprising as CdTe has demonstrated a high propensity for forming it almost irrespective of the substrate surface offered [38]. The resulting interface, however, must overcome the seemingly incompatible situation brought about when the four-fold symmetric substrate surface mates with the six-fold symmetric (1 1 1) plane of CdTe. In this scenario it is reasonable to expect that the resulting in-plane grain structure reflects both a suitable fit to the substrate's atomic arrangement as well as its underlying symmetry. The (1 1 1) pole figure results indicate that this is indeed the case as there exists a four-fold symmetric grain structure which is commensurate with the substrate's cubic crystal structure. The XRD data indicates that these grains are oriented as shown schematically in Fig. 5a. The triangles symbolize the orientation of the (1 1 1) planes on the surface of $SrTiO_3$ represented by the dotted pattern. The arrows on the triangles denote the three equivalent (1 1 1) CdTe planes that project out of its surface. Note that each of these four triangles match poorly to the substrate's lattice constant in all but one direction. In this direction, it is nearly equal to two of the substrate's unit cells (mismatch = 1.6%). This one-dimensional match is preferred to such extents that only grains that comply with it exist within the film. To appreciate the uniqueness of the four grains it should be noted that, for the arrows denoting the (1 1 1) equivalent planes, no two arrows point in the same direction. It is these directions that give rise to the twelve peaks in the outer ring of the (1 1 1) pole figure as is evident from Fig. 5b.

The formation of a [2 1 1] CdTe film on a surface reconstructed (1 0 0) $SrTiO_3$ substrate was quite unexpected. CdTe films with this orientation have been deposited, but only when the interface energy is minimized through the use of [2 1 1] oriented substrates [40–43]. While [2 1 1] substrates provide an appropriate template for [2 1 1] growth, there exist no obvious symmetry arguments that would allow for twelve symmetrically distributed grains to be accommodated on the bulk surface of (1 0 0) $SrTiO_3$. Instead, it is expected that the origin of the [2 1 1] CdTe grains lies with the epitaxial relationship formed between the (2 1 1) planes and the surface reconstruction. In this case, it is expected that the twelve-fold symmetric grain structure is commensurate with the underlying symmetry of the substrate's surface reconstruction. Thus, insight into the nature of the reconstruction is obtained from the observed grain structure. Fig. 6 shows a schematic representation of the (1 1 1) CdTe pole figure where the contributions from each grain are shown. The pole figure's inner ring clearly demonstrates a twelve-fold symmetry in the grain structure as it is comprised of

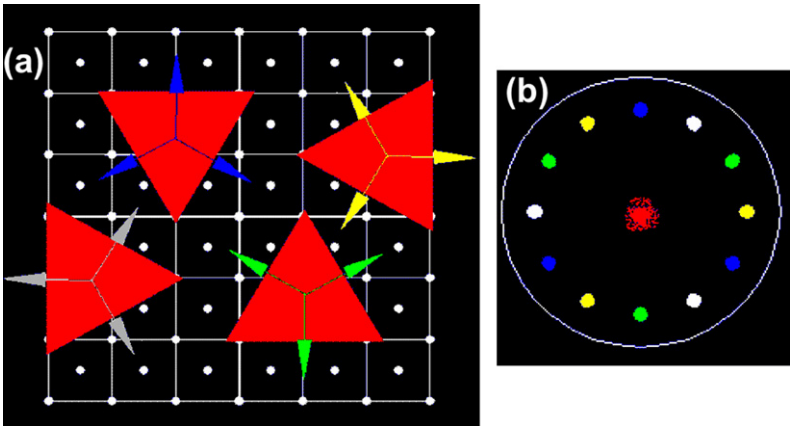

Fig. 5. (a) Schematic illustrating the four possible [1 1 1] CdTe grain orientations (triangles) for films deposited on the $SrTiO_3$ substrate (dotted background). The arrows on each triangle denote the direction of the three equivalent (1 1 1) planes that emerge from the surface. Note that no two arrows are pointing in the same direction. For each grain orientation there exists a one-dimensional geometrical fit (mismatch = 1.6%) to the substrate in either the vertical or horizontal directions. (b) Schematic showing the resulting (1 1 1) pole figure obtained from the four grains where the colour of the dot on the pole figure corresponds to the grain from which it was derived. (For interpretation of the references to colour in this figure legend, the reader is referred to the web version of the article.)

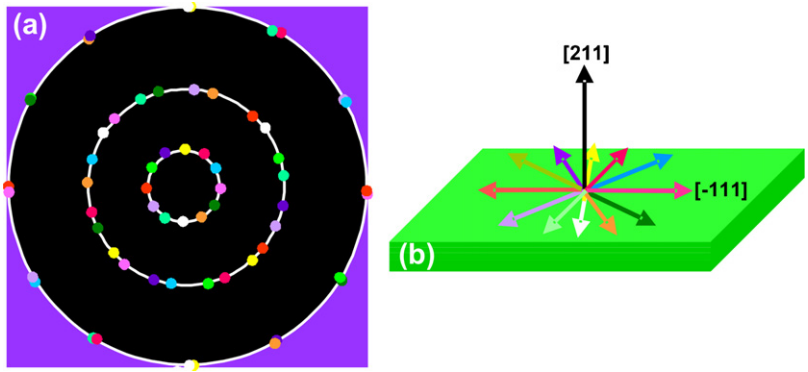

Fig. 6. (a) Schematic detailing the twelve-fold symmetric [2 1 1] CdTe grain structure observed for films deposited on the surface reconstructed substrates. The contribution from each grain is denoted by a different colour. Note that the pattern corresponding to a single crystal [2 1 1] CdTe film (Fig. 3b) is repeated twelve times. (b) Schematic showing the in-plane [−1 1 1] direction for each of the [2 1 1] grains. (For interpretation of the references to colour in this figure legend, the reader is referred to the web version of the article.)

twelve nearly equally spaced peaks where each peak originates from a different grain orientation. Also of significance is the fact that the wide terrace widths shown in Fig. 1b give rise to [2 1 1] CdTe grains even though the film grain size is often smaller than the width of the terrace. Thus, it appears that [2 1 1] grain formation does not rely on nucleation at the substrate steps. This is a strong indication that the atomic scale surface reconstruction is a dominant factor in the promotion of the [2 1 1] grains.

Of the three surface reconstructions known to form in an oxygen ambient, only the $c(4 \times 2)$ and $c(6 \times 2)$ reconstructions present a surface structure where there exist reasonable symmetry arguments able to account for the formation of a [2 1 1] CdTe film having a twelve-fold symmetric grain structure. Such a grain structure must arise from the symmetries of the underlying substrate as it provides the only means for the isolated grains to establish a symmetrical arrangement when first formed in an island growth mode. The (2 1 1) plane of CdTe, shown in Fig. 7, is one-fold symmetric and consists of a series of rows comprised of alternating cadmium and tellurium atoms separated by distances of 8.49 or 2.83 Å. Fig. 8 shows a schematic of the $c(4 \times 2)$ TiO_2 surface reconstruction proposed by Castell [13]. It consists of a series of alternating rows of titanium and oxygen atoms. The top layer has a TiO_2 stoichiometry, but it is sparsely populated with only one quarter the number of atoms present in the TiO_2 layers found in the bulk [13]. With every second row of titanium atoms offset relative to each other they align in a pseudo-six-fold symmetric pattern. Possible geometric fits of the (2 1 1) CdTe plane to this surface reconstruction are shown in Fig. 8b. Each of the three possible geometric fits shown would give rise to two unique grain types due to the one-fold symmetry of the (2 1 1) plane. Six other domain structures would also form by virtue of the fact that the $c(4 \times 2)$ surface reconstruction has two possible domains rotated 90° relative to each other [13]. The domain structure that develops on the reconstructed surface arises from the fact that the rows of titanium atoms have an equal probability of forming along the [0 1 0] or [0 0 1] directions. The net result would be a twelve-fold symmetric [2 1 1] CdTe grain structure. The $c(6 \times 2)$ surface reconstruction, proposed by Jiang and Zegenhagen [18], is shown schematically in Fig. 9. It too is a sparsely populated surface that has the potential to accommodate the (2 1 1) CdTe planes in select directions (Fig. 9b). Here, the four geometrical fits shown give rise to eight unique grain types. In a manner analogous to the $c(4 \times 2)$ reconstruction, the $c(6 \times 2)$ reconstruction also has a domain structure that gives rise to an additional set of eight grains rotated 90° to the ones shown in the figure. An examination of these additional grains, however, reveals that only four of them provide unique solutions as the other four rotate into solutions offered by the first domain. Thus, a twelve-fold $(8 + 8 - 4 = 12)$ symmetric (2 1 1) CdTe grain structure is expected for this surface.

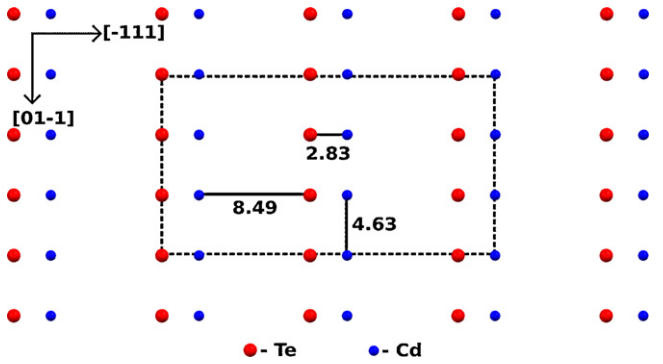

Fig. 7. Schematic of the (2 1 1) plane of CdTe with the interplanar dimensions labeled in units of angstroms. The area outlined by the dashed lines is used in subsequent figures to demonstrate how this structure fits to (1 0 0) $SrTiO_3$ surface reconstructions. The Miller indices shown correspond to the crystallographic orientation of the (2 1 1) CdTe plane.

Assuming that the orientational relationships between CdTe and the surface reconstructions shown in Figs. 8 and 9 are adhered to then it becomes possible to experimentally predict the surface reconstruction undergone by the substrates presented in this work. It should be noted from Fig. 8b that the $c(4 \times 2)$ reconstruction is characterized by (2 1 1) CdTe grain alignment along the substrate's [0 1 0] and [0 0 1] directions. Fig. 4b clearly shows that this is not the case, ruling out this reconstruction for the work presented here. It does not, however, rule out the possibility of [2 1 1] CdTe grain growth if a film were deposited on such a reconstruction. The $c(6 \times 2)$ reconstruction, on the other hand, requires grain growth along the substrate's [0 1 1] and [0 −1 1] directions, consistent with the X-ray data. While we have no direct evidence that the $c(6 \times 2)$ surface reconstruction formed, it is of note that the anneal conditions used elsewhere [18] to obtain this reconstruction are similar to those used here. While it should be understood that predicting a film-substrate orientational relationship solely on the basis of a geometrical fit is somewhat naïve, it is well established that this scenario occurs more often than not.

Even though both the [2 1 1] oriented films show pole figure peaks in similar positions, the relative intensities of the peaks are quite different. This is most easily seen by examining the innermost ring of the pole figure where each of the twelve peaks corresponds to a unique grain orientation. For both samples the

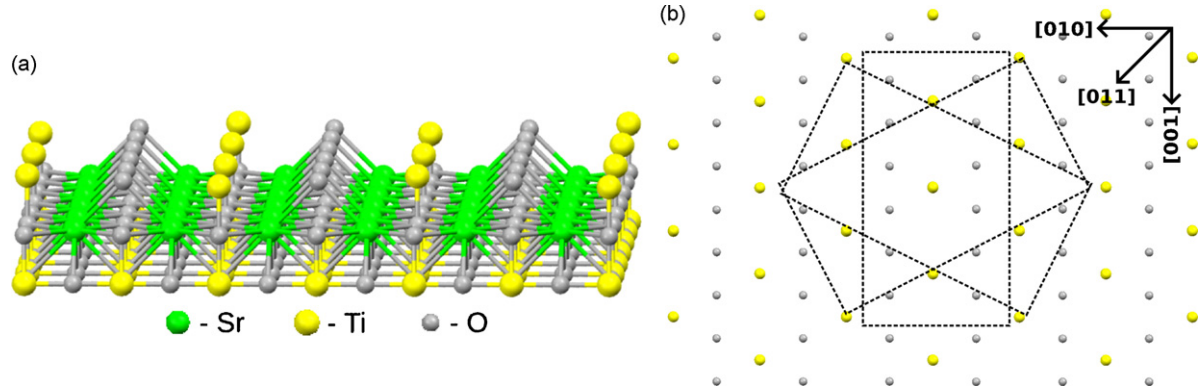

Fig. 8. (a) Schematic showing the surface of the (1 0 0) $SrTiO_3$ with a $c(4 \times 2)$ surface reconstruction. (b) Schematic showing the uppermost layer of the reconstruction with the dashed lines being used to illustrate the closest geometrical fits of the (2 1 1) CdTe plane to this surface. The three orientations shown give rise to six grain orientations as a 180° rotation of the (2 1 1) plane yields a different grain structure. This is a consequence of the fact that the single crystal (1 1 1) CdTe pole figure for a [2 1 1] film is one-fold symmetric (see Fig. 3b). Six other grain structures arise from a domain structure in the substrate surface reconstruction that would be schematically represented by a 90° rotation of Fig. 8b. The Miller indices shown in the top right corner of the figure correspond to the crystallographic orientation of the underlying bulk (1 0 0) $SrTiO_3$ substrate.

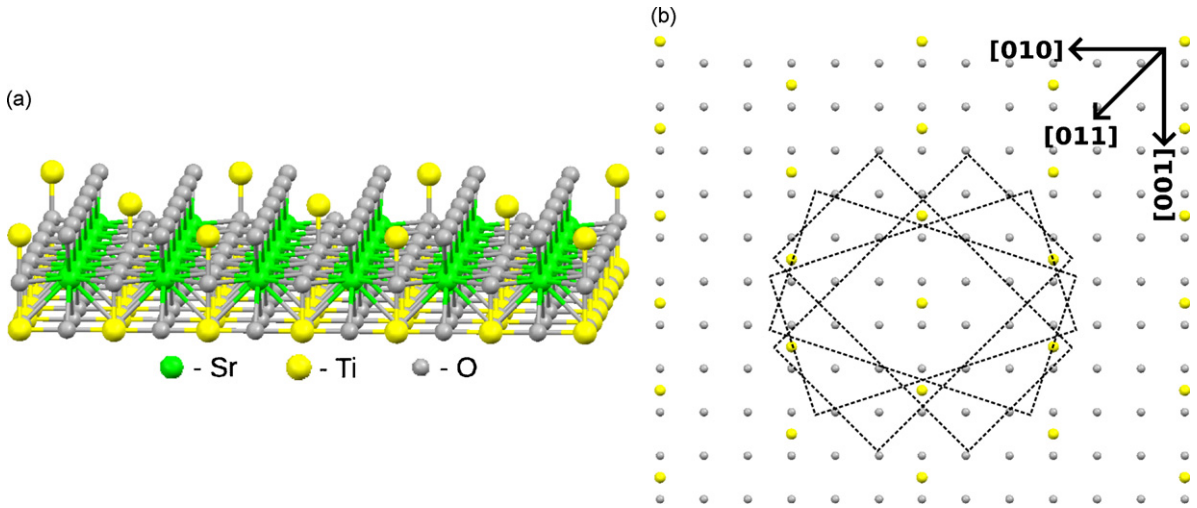

Fig. 9. (a) Schematic showing the surface of the (1 0 0) $SrTiO_3$ with a $c(6 \times 2)$ surface reconstruction. (b) Schematic showing the uppermost layer of the reconstruction with the dashed lines being used to illustrate the closest geometrical fits of the (2 1 1) CdTe plane to this surface. The four orientations shown give rise to eight grain orientations as a 180° rotation of the (2 1 1) plane yields a different grain structure. Eight other grain structures arise from a domain structure in the substrate surface reconstruction that would be schematically represented by a 90° rotation of Fig. 8b. Of these eight grains only four represent unique solutions as the grains forming along the [0 1 1] and [0 1 −1] directions rotate into each other. The Miller indices shown in the top right corner of the figure correspond to the crystallographic orientation of the underlying bulk (1 0 0) $SrTiO_3$ substrate.

peaks on one side of the ring show greater intensities than on the other. This effect, however, is much more pronounced for the pole figure shown in Fig. 4c. Here, the ratio of the integrated intensities between the largest and smallest peak in the ring is 22 compared to 4 for the pole figure shown in Fig. 4b. The fact that the terrace width is approximately four times smaller for the film that shows the most pole figure anisotropy suggests that the step edges promote this preferential grain alignment. Consistent with this explanation is the fact that the highest intensity peaks correspond to the CdTe grain orientation having its [1 1 1] in-plane direction normal to the step. The larger grain sizes exhibited by the surface with smaller terraces are also expected within this scenario. This is a simple consequence of the fact that, in the early stages of film growth, there are more similarly oriented grains that are able to merge into a single larger grain as is expected for an island growth mechanism. With a sizeable effect being observed between the two reconstructed surfaces having a miscut difference of only 0.35°, the potential exists to amplify this effect using a substrate with a significantly larger miscut.

The results presented here demonstrate that the reconstructed surface of (1 0 0) $SrTiO_3$ profoundly alters the grain structure of CdTe films. While it is not unusual for the grain structure to be transformed by the presence of a step-terrace morphology, it is unprecedented for $SrTiO_3$'s atomic-scale reconstructions to promote a film with an alternative heteroepitaxial relationship. For the case of (1 0 0) $SrTiO_3$, there seems to be a disconnect between the research advocating a step-flow growth mode and the wide array of atomic-scale surface reconstructions allowed, with the latter not considered as a determining factor in the film quality achieved. This may be due to the relatively high growth temperatures used in the fabrication of oxide thin films. In this case, the thermal energy available likely facilitates a local rearrangement of surface atoms in response to the addition of adatoms. This is certainly the case for the homoepitaxial growth of silicon where the surface reconstruction gives way to bulk crystalline ordering for temperatures in excess of 300 °C [44]. For the low growth temperatures used in the fabrication of these CdTe films the surface reconstruction is likely locked in place, forcing CdTe to accommodate itself on the reconstructed surface. The sparsely populated nature of such a surface should make it prone to alternative epitaxial relationships as the interface would not consist of an abrupt boundary, but instead, of an amalgamation of two interpenetrating layers. Consistent with this explanation is the fact that different (1 0 0) $SrTiO_3$ surface reconstructions give rise to palladium nanodots having variable orientations and faceting [45].

5. Conclusion

In summary, we have deposited CdTe thin films on both the as-received and reconstructed surfaces of miscut (1 0 0) $SrTiO_3$ substrates. Growth on the as-received substrate yields a [1 1 1] oriented film with four in-plane grain orientations. The reconstructed surfaces, on the other hand, give rise to a grain structure characterized by a [2 1 1] oriented film with a twelve-fold symmetric in-plane grain structure. While it is quite common for a step-terrace reconstruction to alter the in-plane grain structure of a film through the preferential formation of certain grain-types, the radical transformation of the grain structure presented here is unprecedented. We attribute this transformation to an atomic scale surface reconstruction stabilized by the low growth temperatures needed to deposit CdTe thin films.

Acknowledgements

This work is funded by the Natural Sciences and Engineering Research Council of Canada (NSERC), the Canadian Institute for Advanced Research (CIFAR) and the Ontario Research and Development Challenge Fund (ORDCF) under the auspices of the Ontario Photonics Consortium (OPC). The authors would also like to acknowledge the assistance of J.F. Britten, J.D. Garrett and A. Duft.

References

[1] H. Mori, H. Ishiwara, Jap. J. Appl. Phys. 30 (1991) L1415.
[2] R.A. McKee, F.J. Walker, M.F. Chisholm, Phys. Rev. Lett. 81 (1998) 3014.
[3] O.N. Tufte, P.W. Chapman, Phys. Rev. 155 (1967) 796.
[4] A. Ohtomo, H.Y. Hwang, Nature 427 (2004) 423.
[5] W. Siemons, G. Koster, H. Yamamoto, W.A. Harrison, G. Lucovsky, T.H. Geballe, D.H.A. Blank, M.R. Beasley, Phys. Rev. Lett. 98 (2007) 196802.

[6] D. Kan, T. Terashima, R. Kanda, A. Masuno, K. Tanako, S. Chu, H. Kan, A. Ishizumi, Y. Kanemitsu, Y. Shimakawa, M. Takana, Nat. Mater. 4 (2005) 816.
[7] G. Herranz, F. Sánchez, N. Dix, D. Hrabovsky, I.C. Infante, J. Fontcuberta, M.V. García-Cuenca, C. Ferrater, M. Varela, Appl. Phys. Lett. 89 (2006) 152501.
[8] R.L.S. Emergo, J.Z. Wu, T. Aytug, D.K. Christen, Appl. Phys. Lett. 85 (2004) 618.
[9] Y. Ichikawa, T. Matsunaga, M. Hassan, I. Kanno, T. Suzuki, K. Wasa, J. Mater. Res. 21 (2006) 1261.
[10] M.J. Zhuo, Y.L. Zhu, X.L. Ma, H.B. Lu, Appl. Phys. Lett. 88 (2006) 071905.
[11] G.B. Cho, M. Yamamoto, Y. Endo, Y. Shiratsuchi, Y. Kamada, K. Sato, Jpn. J. Appl. Phys. 42 (2003) 6543.
[12] D.S. Deak, F. Silly, D.T. Newell, M.R. Castell, J. Phys. Chem. B 110 (2006) 9246.
[13] M.R. Castell, Surf. Sci. 505 (2002) 1.
[14] N. Erdman, K.R. Poeppelmeier, M. Asta, O. Warschkow, D.E. Ellis, L.D. Marks, Nature 419 (2002) 55.
[15] Q.D. Jiang, J. Zegenhagen, Surf. Sci. 425 (1999) 343.
[16] N. Erdman, L.D. Marks, Surf. Sci. 526 (2003) 107.
[17] N. Erdman, O. Warschkow, M. Asta, K.R. Poeppelmeier, D.E. Ellis, L.D. Marks, J. Am. Chem. Soc. 125 (2003) 10050.
[18] Q. Jiang, J. Zegenhagen, Surf. Sci. 367 (1996) L42.
[19] R. Herger, P.R. Willmott, O. Bunk, C.M. Schlepütz, B.D. Patterson, B. Delley, Phys. Rev. Lett. 98 (2007) 076102.
[20] F. Silly, D.T. Newell, M.R. Castell, Surf. Sci. 600 (2006) L219.
[21] T. Kubo, H. Nozoye, Surf. Sci. 542 (2003) 177.
[22] D.T. Newell, A. Harrison, F. Silly, M.R. Castell, Phys. Rev. B 75 (2007) 205429.
[23] M. Kawasaki, K. Takahashi, T. Maeda, R. Tsuchiya, M. Shinohara, O. Ishiyama, T. Yonezawa, M. Yoshimoto, H. Koinuma, Science 266 (1994) 1540.
[24] T. Nakamura, H. Inada, M. Iiyama, Appl. Surf. Sci. 130 (1998) 576.
[25] G. Koster, B.L. Kropman, G.J.H.M. Rijnders, D.H.A. Blank, H. Rogalla, Appl. Phys. Lett. 73 (1998) 2920.
[26] T. Ohnishi, K. Shibuya, M. Lippmaa, D. Kobayashi, H. Kumigashira, M. Oshima, H. Koinuma, Appl. Phys. Lett. 85 (2004) 272.
[27] G.B. Cho, M. Yamamoto, Y. Endo, Jpn. J. Appl. Phys. 43 (2004) 1555.
[28] G.B. Cho, Y. Kamada, M. Yamamoto, Jpn. J. Appl. Phys. 40 (2001) 4666.
[29] G.B. Cho, M. Yamamoto, Y. Endo, Thin Solid Films 464 (2004) 80.
[30] Y. Xin, N.D. Browning, S. Rujirawat, S. Sivananthan, Y.P. Chen, P.D. Nellist, S.J. Pennycook, J. Appl. Phys. 84 (1998) 4292.
[31] H. Nishino, Y. Nishijima, J. Cryst. Growth 167 (1996) 488.
[32] Y.P. Chen, J.P. Faurie, S. Sivananthan, G.C. Hua, N. Otsuka, J. Elec. Mater. 24 (1995) 475.
[33] I. Sugiyama, Y. Nishijima, Appl. Phys. Lett. 66 (1995 2798).
[34] Y.P. Chen, S. Sivananthan, J.P. Faurie, J. Elec. Mater. 22 (1993) 951.
[35] R. Sporken, Y.P. Chen, S. Sivananthan, M.D. Lange, J.P. Faurie, J. Vac. Sci. Technol. B 10 (1992) 1405.
[36] R. Sporken, M.D. Lange, C. Masset, J.P. Faurie, Appl. Phys. Lett. 57 (1990) 1449.
[37] R. Sporken, S. Sivananthan, K.K. Mahavadi, G. Monfroy, M. Boukerche, J.P. Faurie, Appl. Phys. Lett. 55 (1989) 1879.
[38] S. Neretina, Q. Zhang, R.A. Hughes, J.F. Britten, N.V. Sochinskii, J.S. Preston, P. Mascher, J. Electron. Mater. 35 (2006) 1224.
[39] C. Reig, N.V. Sochinskii, V. Muñoz, J. Cryst. Growth 197 (1999) 688.
[40] M.D. Lange, R. Sporken, K.K. Mahavadi, J.P. Faurie, Y. Nakamura, N. Otsuka, Appl. Phys. Lett. 58 (1991) 1988.
[41] A. Million, N.K. Dhar, J.H. Dinan, J. Cryst. Growth 159 (1996) 76.
[42] S. Rujirawat, L.A. Almeida, Y.P. Chen, S. Sivananthan, D.J. Smith, Appl. Phys. Lett. 71 (1997) 1810.
[43] J.P. Zanatta, P. Ferret, P. Duvaut, S. Isselin, G. Theret, G. Rolland, A. Million, J. Cryst. Growth 184/185 (1998) 1297.
[44] H.-J. Gossmann, L.C. Feldman, Phys. Rev. B 32 (1985) 6.
[45] F. Silly, M.R. Castell, Phys. Rev. Lett. 94 (2005) 046103.